SSRG International Journal of Electrical and Electronics Engineering
ISSN: 2348-8379/ https://doi.org/10.14445/23488379/IJEEE-V11I8P117

Volume 11 Issue 8, 188-207 August 2024

Original Article

AI Based Hybrid Controlled Grid / Standalone Solar Integrated Unified Power Quality Conditioner for the EV Charging Station

Bomma Shwetha[1], G. Suresh Babu[2], G. Mallesham[3]

[1]*Electrical Engineering Department, University College of Engineering, OU, Telangana, India.*
[2]*Electrical & Electronics Engineering Department, CBIT, Telangana, India.*
[3]*Electrical Engineering Department, University College of Engineering, OU, Telangana, India.*

[1]*Corresponding Author : bomma.swetha243@gmail.com*

Received: 07 June 2024 Revised: 11 July 2024 Accepted: 08 August 2024 Published: 31 August 2024

Abstract- *Grid-connected sustainable systems are now increasingly vulnerable to PQ problems due to the development of power electronics technology. In actuality, there are two instances in which Electric Vehicle Charging Stations (EVCS) have significant distortions: (1) when they are connected to the grid and (2) when they are operating independently and receiving power from BESD and solar energy. It must be addressed immediately to resolve this and enable the system's Power Quality upgrade. A hybrid control method, which combines a PIC for the SHPF of the Unified PQ Conditioner (UPQC) with an Artificial Neural Fuzzy Interface System (ANFIS), is suggested for the current UPQC to improve the PQ level. Attaining steady SVDC during variations in loads and sun irradiation changes is the primary objective of UPQC. Other objectives include mitigating disturbance/ swell/ sag and grid voltage imbalances. The developed model's working using grid and island scenarios is assessed using four distinct test cases. To prove its superiority, it is necessary to compare the suggested technology against industry standards like SMC controllers and Proportional Integral Controllers (PIC). The proposed methodology reduces THD to 2.23%, 2.28%, and 1.84%; nonetheless, it is not as effective as the existing methods indicated by the survey.*

Keywords - *Artificial Neuro Fuzzy Interface System, PV system, UPQC, EV charging station, Power quality.*

1. Introduction

Devices linked to the power supply may experience malfunction, data loss, or damage due to PQ problems. Ensuring optimal power quality is not just a matter of convenience but a crucial necessity, particularly in delicate settings such as medical facilities. To maintain a high PQ for customers, utility providers must also guarantee a steady and dependable power distribution system. Furthermore, a key first step in developing a more ecologically friendly and sustainable energy system is the integration of renewable sources into distribution networks.

However, the erratic and fluctuating nature of clean sources generates a number of complications for this integration. The most important PQ issue of all is THD. Higher THD can result in problems like electrical equipment overheating, communication system interference, and decreased system efficiency. Hence, lower THD values are desirable and imperative for electrical systems. Minimal THD must be maintained for optimal PQ and effective equipment functioning in power systems. Therefore, electrical designers' top priority now is to guarantee PQ stability.

1.1. Literature Review

Using UPQC techniques and control methodologies to augment PQ proposes an adaptable control scheme to augment efficacy. The proposed dynamic regulation method enhances behavior on a critical three-phase system under study [1]. The control approach employs a PLL mechanism to avert significant zero exceeds at severely distorted supply voltage monitoring [2]. The UPQC enhances power quality by ensuring the supply current and output voltage remain sinusoidal at the desired voltage levels. Additionally, it reduces voltage in addition to current defects by suppressing the harmonics and load side current irregularities [3].

Nonetheless, the UPQC device's compensating capabilities are enhanced by the recommended control technique, reference DC link voltage management and ANFIS for DC voltage management. An offline-trained ANFIS is used in the online simulation. [4]. In addition, BESD for the UPQC and Fourier conversion were created for clean energy to lessen voltage swings and flaws in the load current [5]. Real-time generation of a benchmark dataset was achieved across several PQ scenarios. Based on the gathered data, a

deep-learning intelligent controller model was developed, and it now controls the system to guarantee a continuous and reliable power supply. [6].

By employing an ANFIS control technique, the unified PQ conditioner has been selected to handle imperfections. Furthermore, it improves the network's functionality [7]. To handle and alleviate PQ difficulties, the FLC was specifically created for SEAF [8]. The ACO technique has been released to maximize the PIC's gains and reduce THD for the SHPF under varied load scenarios [9]. The developed system was examined using the ANFIS approach. The Fuzzy controller uses language to determine system parameters, which improves system efficiency and helps provide current benchmarks [10].

A flexible FLC is specifically designed to adapt to changes in system parameters. UPQC is intentionally exposed to nonlinear switching and static stresses to reduce voltage swings, sag/swell, and eliminate harmonics [11]. An optimized GA-based ANFIS was presented to adjust the system's DLV and PQ problem. Thus, the recommended technique maintains DC bus voltage regulation [12].

A powerful UPQC, which is frequently used in conjunction with conventional sources, is considered in the microgrid design offered to control the flow of electricity. The ANFIS methodology has been utilized to enhance its optimization [13]. The overall cost of the system was minimized by developing ANN-based control to distribute power across the converters without increasing the VSC specifications [14].

The Multi-Converter UPQC utilizes two series VSCs to transfer power between feeders by employing a hybrid approach that combines two metaheuristic algorithms-the Beetle Swarm Optimization and Butterfly Optimization Algorithm. This method effectively eliminates transients, voltage sags, swells, and interruptions from the system [15]. Besides, the PQ was improved by integrating the Path Finder for optimal UPQC placement and sizing [16]. Output current harmonics are managed by the EVCS-based UPQC-SMES system.

Additionally, a UPQC integrated with the Superconducting Magnetic Energy Storage (SMES) system was developed specifically for EVCS to address grid voltage disturbances [17]. This work suggests a micro-grid system incorporating renewable energy using UAPF. This is where the UAPF DC-link combines the BSS with clean sources, such as solar and wind [18]. To mitigate current distortions in current and harmonics, a new PIC based on the Automatically Updating-Sparrow Search optimization is recommended [19].

A novel control strategy for the enhanced UPQC compensating capabilities was introduced during sag situations, the fixed gain PIC utilized in conventional approaches may raise error between the actual and set DC bus voltage [20]. To successfully address PQ problems, renewable sources are used based on artificial intelligence control approaches for SHPF and UPQC [21-26]. Similarly, the non-conventional sources fed SHPF and UPQC, optimally developed PIC, and NN controls were recommended as an additional method to filter the choice of filter parameters through the use of metaheuristic techniques [27-36].

Table 1. State of the art of survey (literature)

Ref no		PQ problems				Loads		
	Control Adopted	Total Harmonic Distortion	DC bus voltage balancing	Grid Voltage sag, swell	Grid Voltage disturbance	Harmonic balanced	Un-balanced	EV charging station
[11]	Fuzzy	X	X			X		
[12]	Neuro fuzzy	X		X	X	X	X	
[13]	Neuro fuzzy	X	X	X	X	X		
[14]	Neural Network	X		X	X	X		
[17]	PI	X		X	X	X	X	X
[19]	PIC, in association with SSA	X		X	X			
[20]	Neuro fuzzy with PI	X		X	X	X	X	
Developed Method	ANFIS-PIC	X	X	X	X	X	X	X

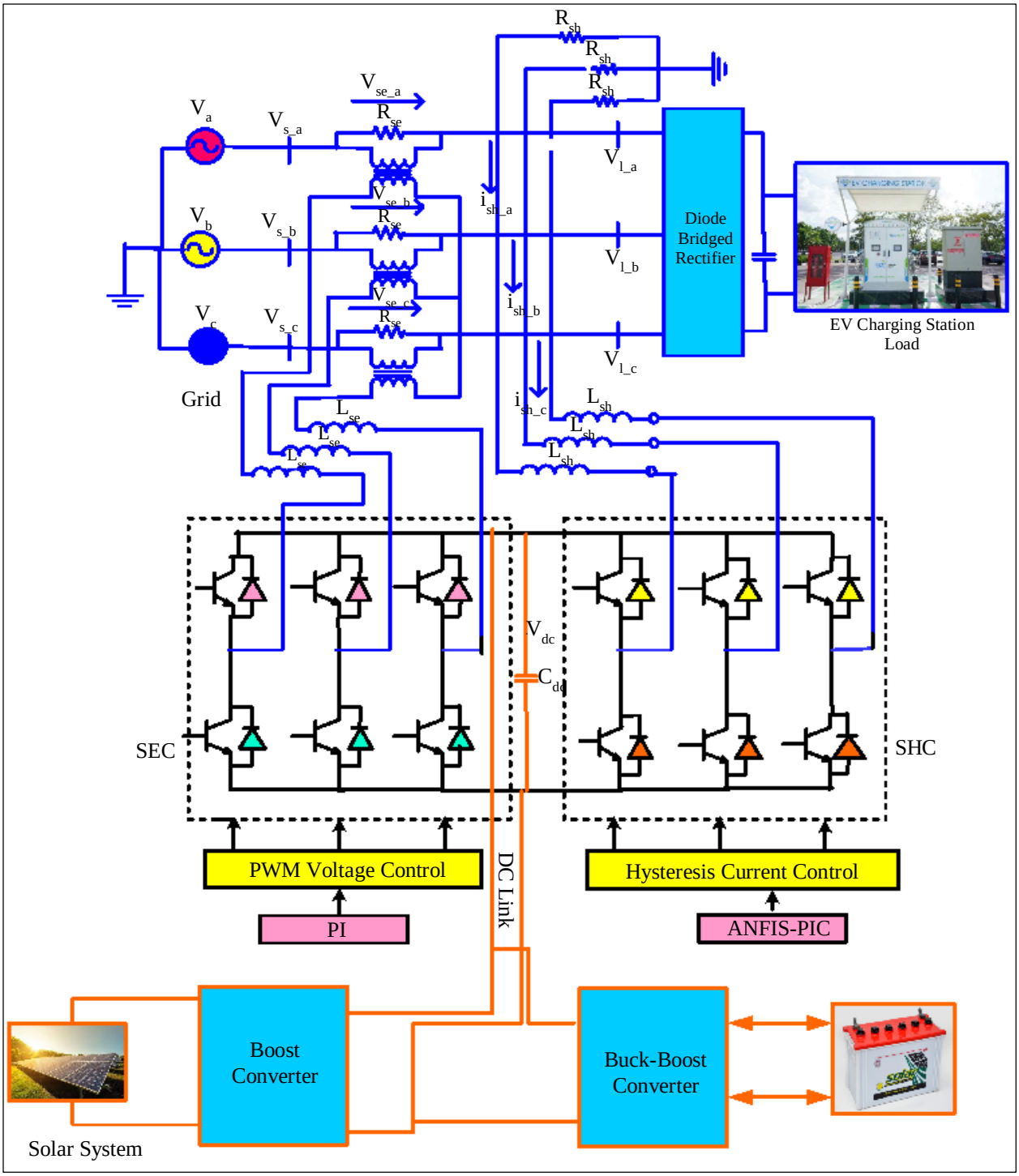

Fig. 1 Developed UPQC

1.2. Novelty

Table 1's literature indicates that numerous studies have primarily focused on addressing a single goal at a time. In contrast, the goal of this work is to handle multiple PQ issues under various conditions, such as solar radiation, EV charging, and both in-phase and unequal phase grid voltage scenarios, for both standalone and grid-integrated systems with several loads as test cases. The following are the manuscript's main contributions:

- The development of a hybrid controller known as ANFIS-PIC containing characteristics of both ANFIS and proportional integral is proposed for the UPQC to manage both the EVCS and station base load.

- The primary objective of the solar and energy storage-powered UPQC is to reduce THD, stabilize SVDC under load and varying solar irradiance, and compensate for voltage harmonic disturbances, as well as mitigate swell and sag conditions.
- The working of the controller is evaluated through four cases across two different scenarios (grid-interconnected and standalone). These studies consider various combinations of loads, partial shading due to solar irradiation, voltage phase imbalance in the grid, and other related factors.
- To demonstrate the superiority of the developed system, a comparative study is conducted against well-established methods such as PI and FLC, along with other techniques available in the scientific literature.

1.3. Alignment of Paper

Section 2 gives the developed configuration. However, Section 3 discusses the ANFIS-PIC for the VSC, Section 4 provides the converters, and finally, Section 5 analyzes the findings. Section 6 concludes with the study's findings

2. Proposed Test System

Figure 1 gives the structure of the UPQC integrated PV system. The UPQC and the SPVS with BESD are connected through a DC bus. A SEAF and a SHAF comprise the UPQC. SEAF aims to reduce voltage swings by supplying the required compensating voltage. Moreover, a transformer is used to isolate VSCs and the supply line. In addition, SHAF's primary goal is to suppress the harmonics in signals and regulate SVDC. For both balanced and unbalanced loads, a three-phase rectifier was chosen.

2.1. PV and Battery Modelling

In the suggested system, the clean energy PV source with storage battery helps to DC bus voltage stable under the condition of fluctuation in load with partial shading condition in addition to the reduction of burden on converters.

2.1.1. SPVS

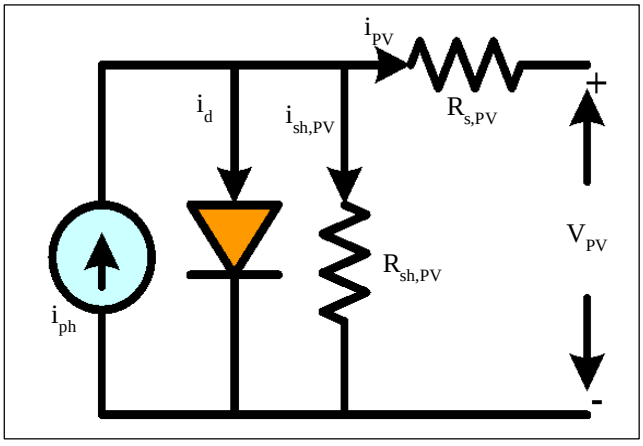

Fig. 2 PV model

As seen in Figure 2, single diode based PV cell. The PV cell detects the i_{ph} from sunlight and converts it into electrical power. The current output is obtained by using KCL, as shown in Equation (1).

$$i_{PV} = i_{ph} - i_d - i_{sh} \tag{1}$$

In the present work, we utilize incremental conductance MPPT and apply Equation 4 to obtain the highest possible output. The control circuit is given in Figure 3.

$$i_{PV,m} = i_{ph}N_p - i_{S,PV}N_p\left[\exp\left(\frac{Q\left(V_{PV}+\frac{N_S}{N_P(i_{PV,m}R_{S,PV})}\right)}{N_S\eta kT_C}\right)-1\right] - \frac{V_{PV,m}+N_S/N_p(i_{PV,m}R_{S,PV})}{N_S/N_P(R_{sh,PV})} \tag{2}$$

Where,

$$i_{ph} = (i_{ph,n} + K_1\Delta T_C)\frac{G}{G_n} \tag{3}$$

$$P_{PV} = V_{PV}xi_{PV} \tag{4}$$

For PV systems, the ICM based MPPT approach maximises output. This is accomplished by the ICM, which continually modifies the PV system's operating point to monitor changes in the surrounding environment and guarantee maximum power output. The operating point adjustment direction is determined by the algorithm by comparing the ICM to a reference value. Figure 4 displays the ICM flow chart. When faced with dynamic and quickly changing variables, like variations in temperature and solar irradiation, the Incremental Conductance Method is renowned for detecting the maximum power point quickly and accurately. Under some circumstances, it could show oscillations around the MPP, which can be fixed by utilizing further control techniques or hysteresis. The choice of the MPPT algorithm is contingent upon various aspects, including system complexity, cost, and performance requirements. Each method has pros and cons.

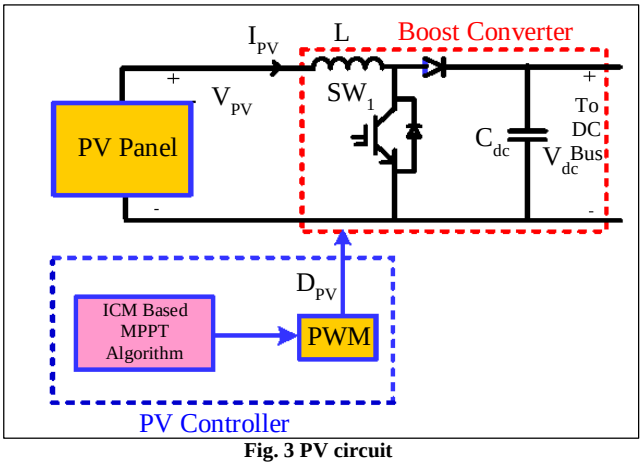

Fig. 3 PV circuit

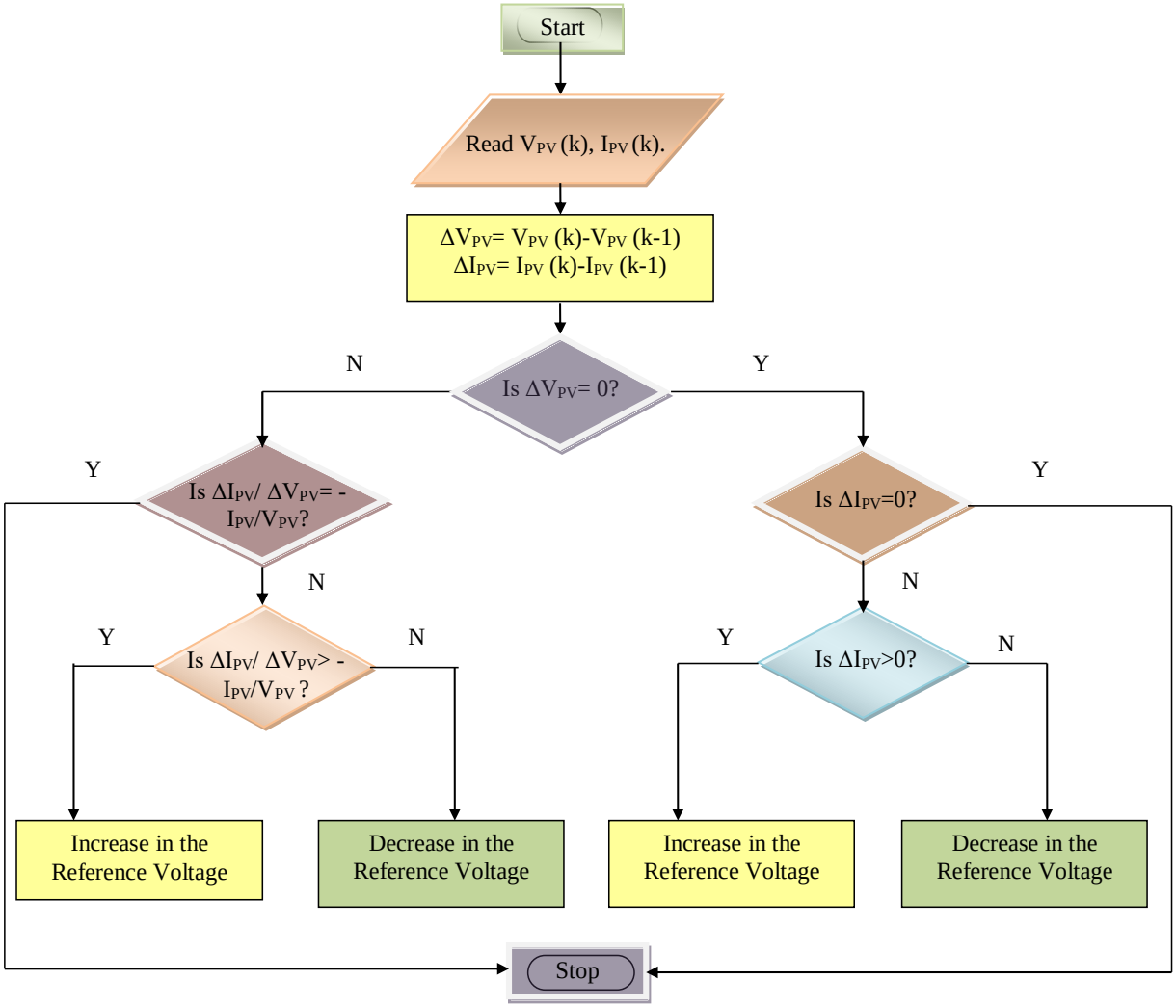

Fig. 4 Flow chart of ICM based MPPT

2.1.2. Battery Storage

The Li-ion type storage battery includes a variety of benefits like very slow in release and a lesser service. Switches SW_1 and SW_2 can charge or drain the battery, as shown in Figure 5(a). The battery state can be calculated by Equation (5).

$$SOCB=60(1+\int i_{BS}dtQ) \quad (5)$$

Equation (6) states that the amount of SPS the SOCB limit determines whether the battery is charging or discharging. In this case, Q and i_{ref} stand for battery charge, real current, and reference current, whereas SOC_{max} and SOC_{min} indicate the maximum and lowest values allowed for SOCBs. Batteries with voltage, capacitance, and inductance denoted by "V_B," "C_B," and "L_B." Finally, the determined and set DC capacitor voltages are V_{dc} and V^{ref}_{dc}. Figure 5(b) shows the required DC link voltage in the battery operation control circuit. Table 2 includes the recommended operating modes for the system, whereas Table 1 lists the solar with energy storage specifications selected in this work.

$$SOCB_{min} \leq SOCB \leq SOCB_{max} \quad (6)$$

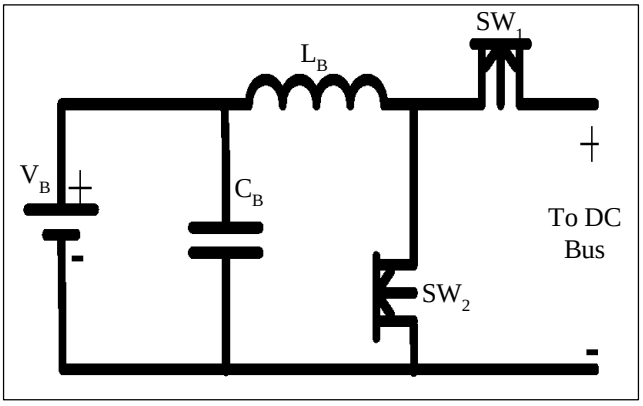

(a) ESS configuration at DC link

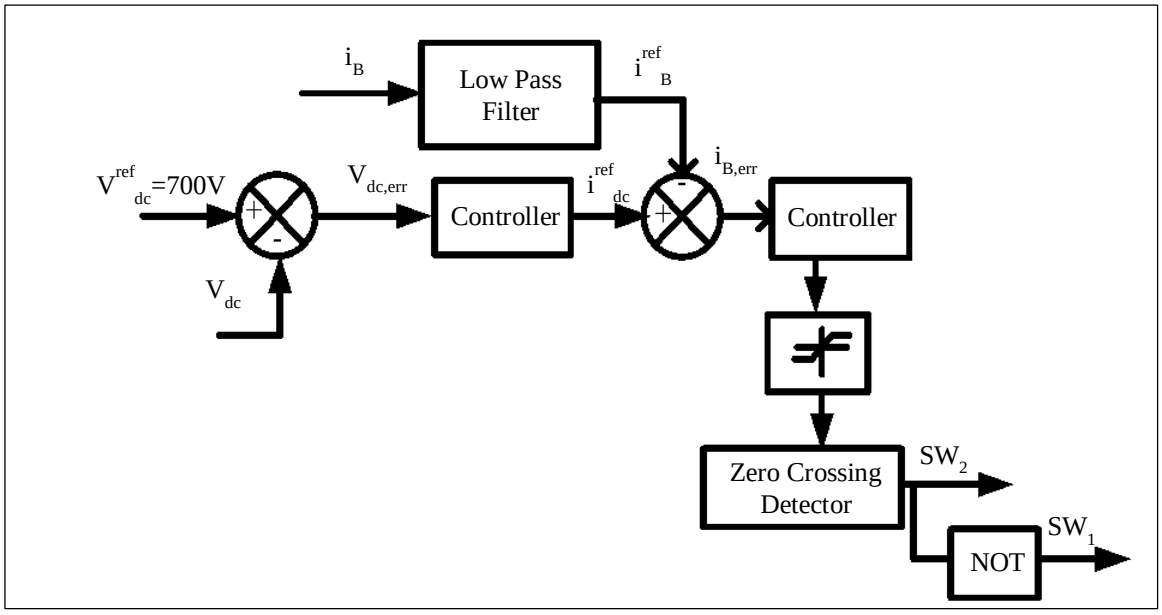

(b) ESS controller
Fig. 5 ESS control

Table 2. Working modes

State	Steps
Mode-1: Grid integrated	In association with clean energy, and storage grid will feed the EV
Mode-2: islanded state	Clean energy will feed EV

3. Shunt Converter

The primary goal of SHAF is to lessen the imperfections in the current waveforms by adding the proper compensatory current and maintaining the SVDC constant. The model performs (i) dq0/abc conversions; (ii) ANFIS-PIC is built to obtain the required objectives.

Figure 9 shows the SHAF control system with the suggested method. Since the literature review already discusses and offers details on conversions, the suggested ANFIS-PIC control strategy will be described below.

3.1. ANFIS-PIC for SVDC

The voltage management of the DC link capacitor is handled by the ANFIS-PIC. E and the rate of CE are accepted as inputs by the ANFIS, and an output is produced by NN. As shown in Figures 6(a) and (b), triangular membership is used to describe the FLC's error and change in error, respectively. The symbols for the linguistic variables are "PB," "PM," "PS," "ZO" (zero), "NM," "NB," and "NS." The linguistic characteristics listed in Table 3 are used to develop fuzzy "IF-THEN" rules. Here, increasing the rules can improve accuracy; however, it also makes the system more complex.

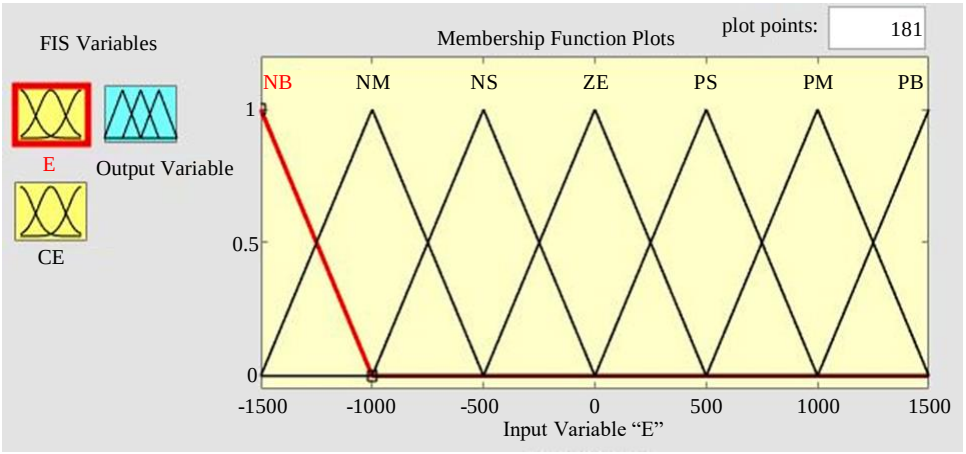

(a) E

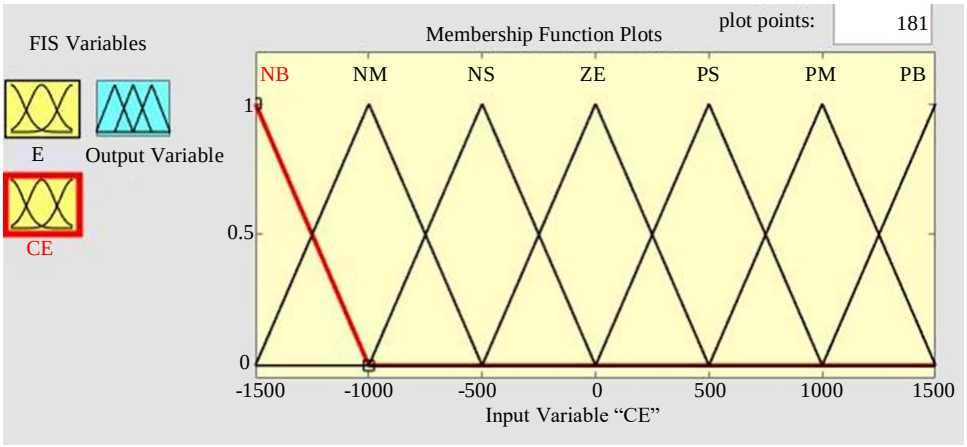

(b) CE

Fig. 6 MESF

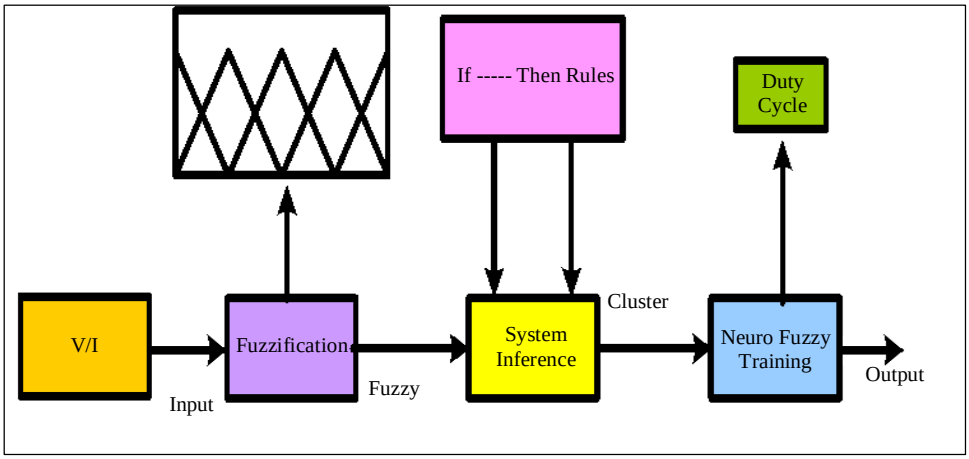

Fig. 7 Overview of ANFIS

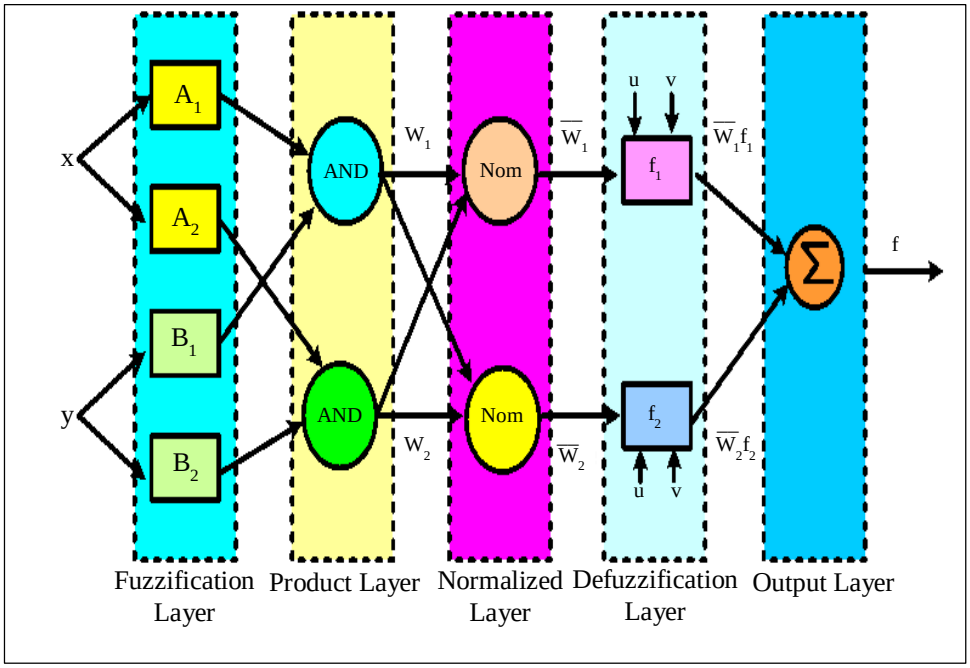

Fig. 8 Structure of ANFIS

However, the firing strength w_i is calculated in the second layer using the AND operator, and the MSF got by the first layer, the output is given by Equation (7).

$$w_k = \mu_{Ai}(x) * \mu_{Bj}(y) \;\; i,j = 1,2 \tag{7}$$

Values are normalized in the next layer, where data is obtained from the layer before it. Every node comes to normalization through computing the relation of the total strength of firing of all the rules with the firing strength for the k^{th} rule, as given by Equation (8).

$$\overline{w_k} = \frac{w_k}{w_1+w_2} k = 1,2 \tag{8}$$

The ANNC may adjust to itself by employing the defuzzification in the fourth layer with inference parameters $(p_k, q_k, r_{k)}$. Equation (9) provides the outcome of this operation.

$$\overline{w_i} f_i = \overline{w_i}(p_k u + q_k v + r_k) \tag{9}$$

In order to obtain the necessary total ANFIS output, all the inputs are added at the fifth layer using Equation (10).

$$f = \sum_i \overline{w_i} f_i \tag{10}$$

Figure 10 shows the inner structure of the ANFIS, whereas Figure 8 shows a schematic figure of the ANFIS. Pharos is used to transform the electrical current into a dq domain, and PLL is used by the supply voltage to control the frequency. The VADLC must be controlled, and the reference current must be generated for the SHAF to function.

However, power flow may change in response to variations in electrical demand, which would result in changes in the VADLC. A DC error signal is introduced by the proposed ANFIS-PI controller and is found by comparing the reference and real DLV using Equation 11.

$$\Delta i_{dc} = e_1(t) = V_{dc}^{ref} - V_{dc}(t) \tag{11}$$

The dth component of the i_l is increased by the error signal from the ANFIS-PIC. The dq components are shifted into an abc and compared with i_l at the hysteresis control to produce the necessary gate signals. In Figure 9, the suggested controller is shown.

4. Series Controller

By comparing the voltage across the load, which is converted into a frame, the controller produces signals. Later on, it is changed into a frame, as seen in Figure 10. A PWM control generates the pulses.

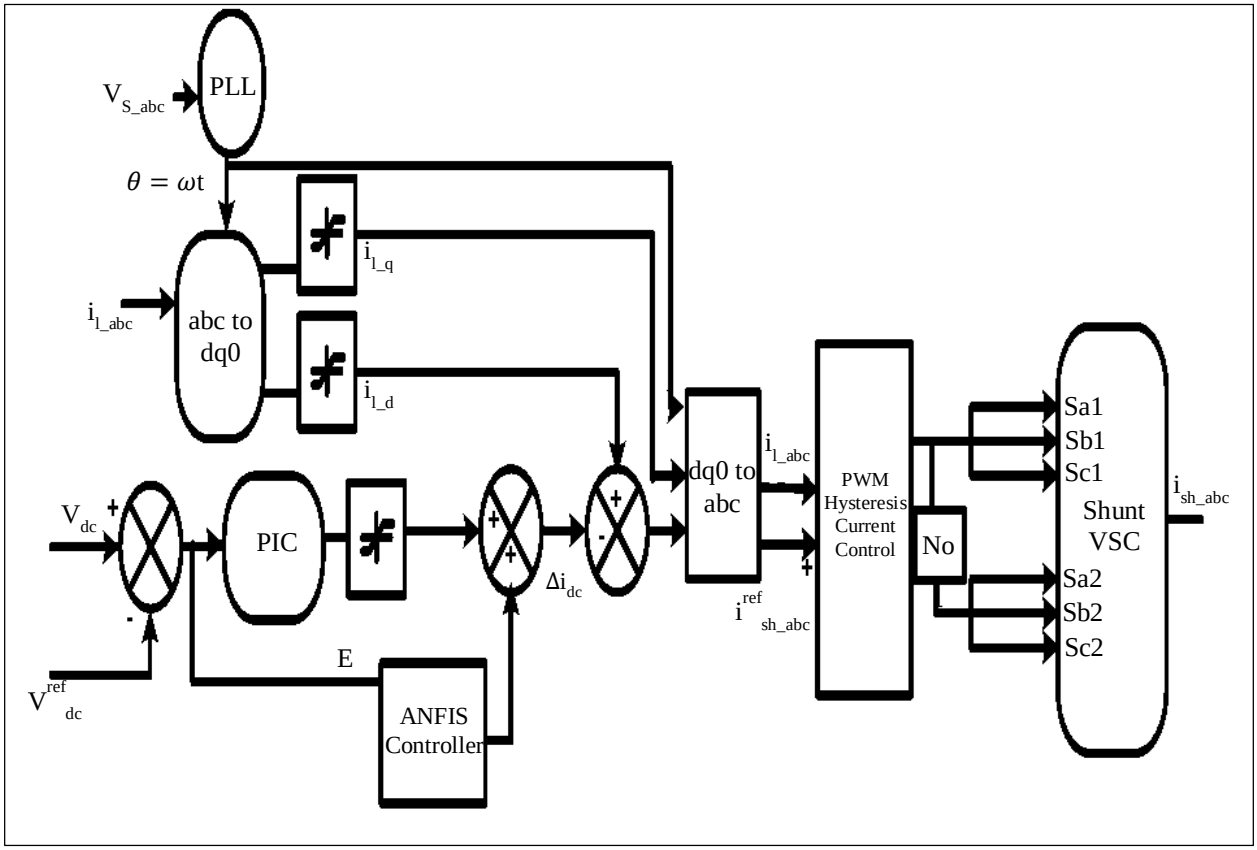

Fig. 9 Hybrid controller for shunt converter

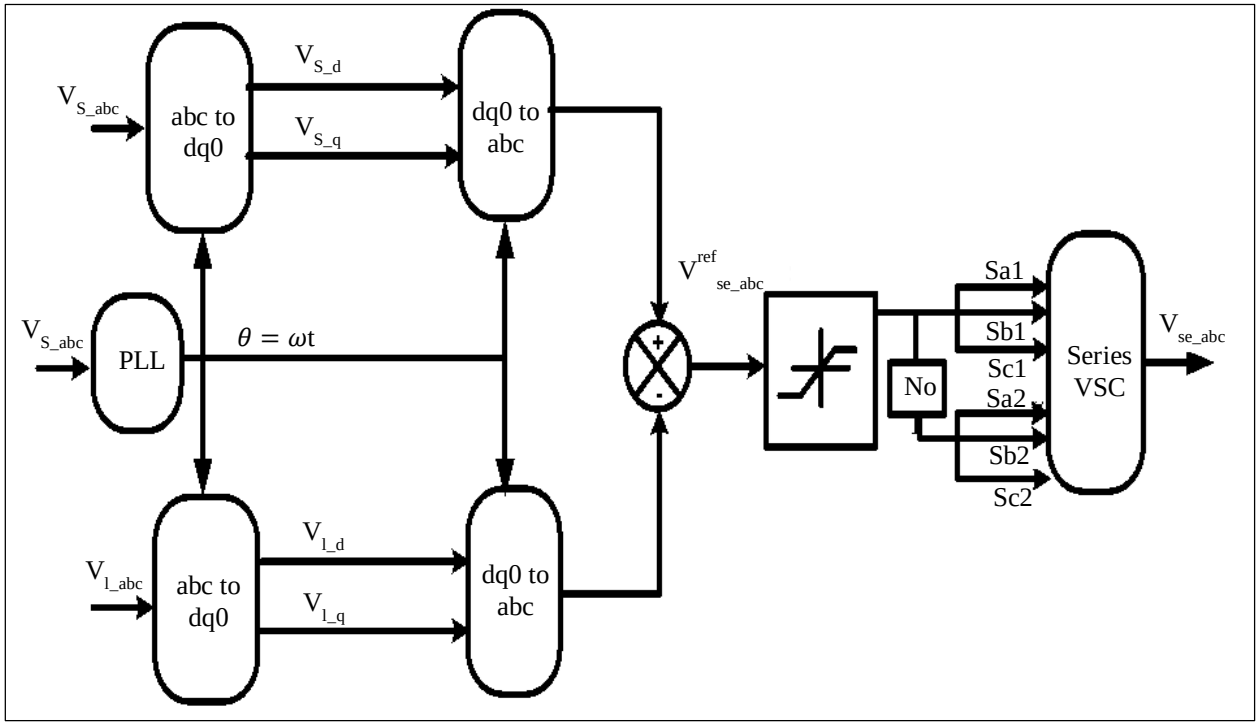

Fig. 10 Series converter control system

5. Results Analysis with Discussions

The three-phase system is chosen to verify the proposed hybridized controller. The Matlab 2016 software was used to generate the recommended strategy. The developed system and its load values are provided in Appendix 1.

Two test scenarios (Grid and island conditions) with four case studies illustrate the enhanced performance of the built ANFIS-PIC on the UPQC. Various combinations that involve different types of loads and conditions, like PQ issues with constant and variable solar panel array irradiation, are examined in this research.

The source voltages are considered balanced in test studies 1, 2, and 3, while they are unbalanced in test study 4. In each case, the THD was calculated using Equation 12, and the outputs were compared with standard SMC and PIC methods, in addition to various approaches discussed in the introduction, as shown in Table 3.

$$THD = \frac{\sqrt{\sum_{n-1}^{N} I^2 n}}{I_f} \quad (12)$$

While I_f resembles the signal's fundamental element, In represents the n^{th} order harmonic component. In case 1 for scenario-1, the V_S with 30% of swell and sag at the designated time periods of 0.25-0.35sec and 0.4 to 0.5sec, etc., as shown in Figure 11(a). However, when combined with PV and storage systems, UPQC can identify voltage abnormalities, inject a suitable V_{se}, and maintain a stable magnitude of load voltage. The performance of SHAF has been examined in relation to an EV charging station using rectifier-bridged harmonic load.

It was identified that the i_l was in phase but distorted, as seen in Figure 11(b). The developed approach reflects the decrease in THD by lowering current signal flaws. Furthermore, as indicated in Table 4 [citation provided], the present THD has decreased to 2.23%, which is significantly less than the other approaches found in the study survey. Additionally, as seen in Figure 11(c), the VADLC steady value of 700V underwent a little 0.05 seconds.

Similar to example 1, balanced Vs is selected in case 2, but with distortions in supply voltage, as illustrated in Figure 12(a). However, the developed approach maintains a constant voltage between the load terminals. Because of the pq load that was taken into account in addition to the EV charging station load, the i_l is identified to be sinusoidal with equal phases, as shown in Figure 12(b).

With the recommended approach, THD is lowered to 2.28%. Clearly, the proposed method effectively addresses PQ problems related to both *Vs* and i_l. But as Figure 12(c) demonstrates, even with simultaneous changes in the load and irradiation, the recommended controller maintains the V_{dc} at 700V for a short while (0.02 seconds).

Table 3. Test cases considered

Condition / Load	Case1	Case 2	Case3	Case4
	Scenario-1 (Grid integrated)			Scenario-2 (stand-alone)
Load no: 1 (Rectifier)	✓		✓	✓
Load no: 2 (p & q)		✓		
Load no: 3 (unequal phases)			✓	
Load no: 4 (EV)	✓	✓	✓	✓
Standard sun irradiation	✓			✓
Variation in sun irradiation		✓	✓	
Grid supply with balanced phases	✓	✓		✓
Grid supply with unbalanced phases			✓	
Sag and swell in grid voltage	✓			
Disturbance in grid voltage		✓		
Current THD	✓	✓	✓	

Table 4. % THD comparison

Controller		Case-1			Case-2			Case-3		
		Phase-a	Phase-b	Phase-c	Phase-a	Phase-b	Phase-c	Phase-a	Phase-b	Phase-c
PI	LV	2.44	2.49	2.65	2.49	2.54	2.69	2.51	2.59	2.74
	SC	2.68	2.97	3.33	3.15	3.38	4.18	2.74	2.92	3.43
SM	LV	2.25	2.62	2.22	2.39	2.37	2.52	3.44	3.16	3.01
	SC	2.74	2.52	2.97	3.26	3.99	3.16	2.92	2.92	2.65
PI[9]	LV	--	--	--	--	--	--	--	--	--
	SC	3.8	--	--	--	--	--	--	--	--
PI[5]	LV	--	--	--	--	--	--	--	--	--
	SC	3.4	--	--	--	--	--	--	--	--
PI[7]	LV	--	--	--	--	--	--	--	--	--
	SC	14.7	--	--	--	--	--	--	--	--
ANFIS[7]	LV	--	--	--	--	--	--	--	--	--
	SC	6.1	--	--	--	--	--	--	--	--
PI[8]	LV	--	--	--	--	--	--	--	--	--
	SC	2.4	--	--	--	--	--	--	--	--
FL[8]	LV	--	--	--	--	--	--	--	--	--
	SC	3.6	--	--	--	--	--	--	--	--
ANFIS-PI	LV	**2.27**	**2.31**	**2.33**	**2.28**	**2.31**	**2.32**	**2.08**	**2.08**	**2.07**
	SC	**2.23**	**2.37**	**2.93**	**2.28**	**2.40**	**3.04**	**1.84**	**2.05**	**2.41**

**Note: LV= Load voltage; SC= Source current*

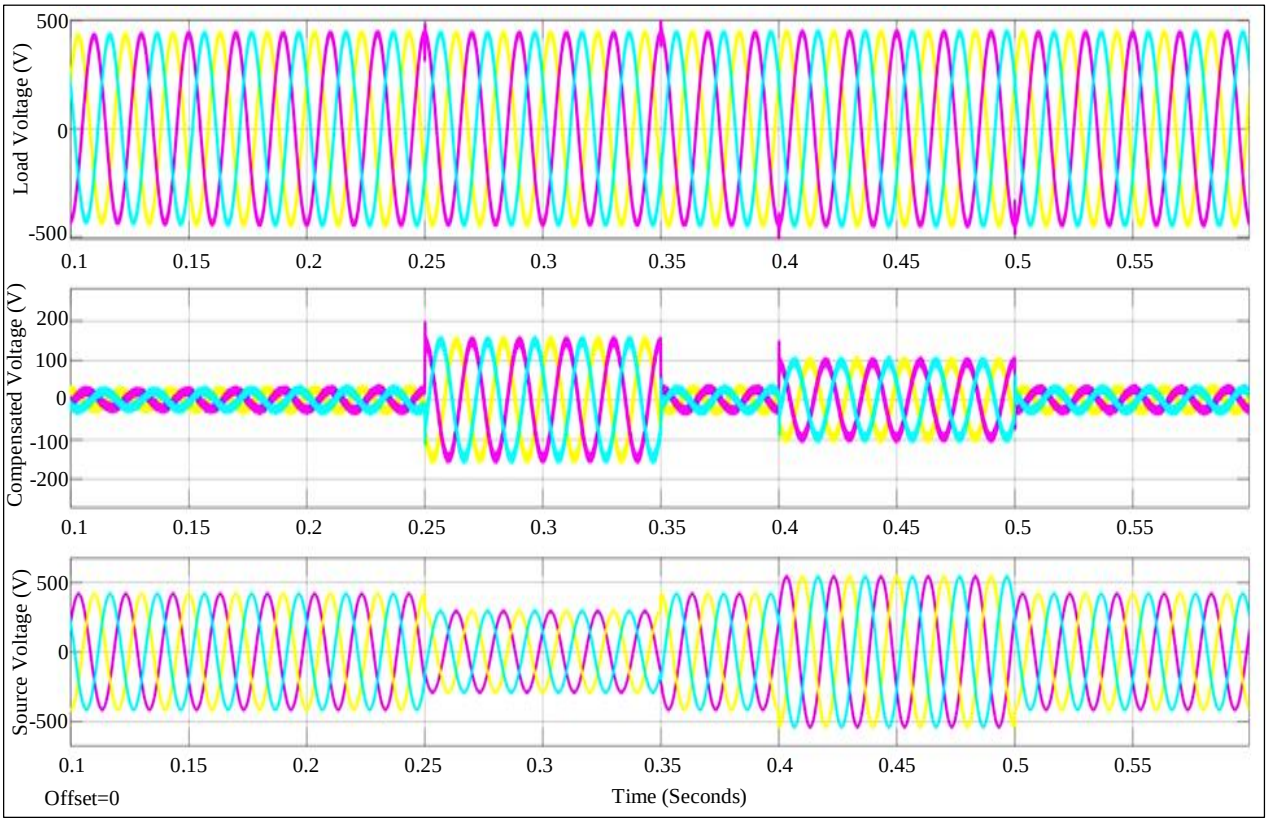

(a) Source, injected and demand voltages

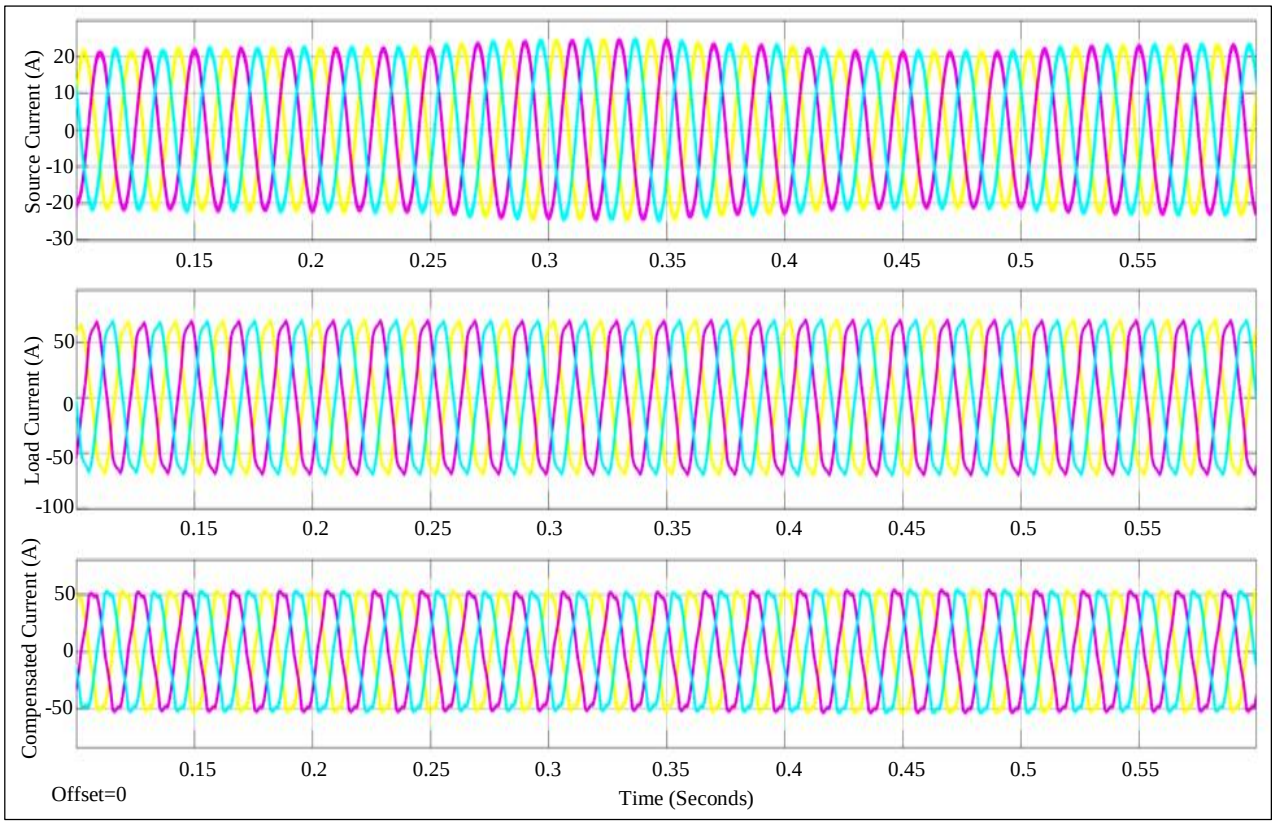

(b) Source, demand, and injected currents

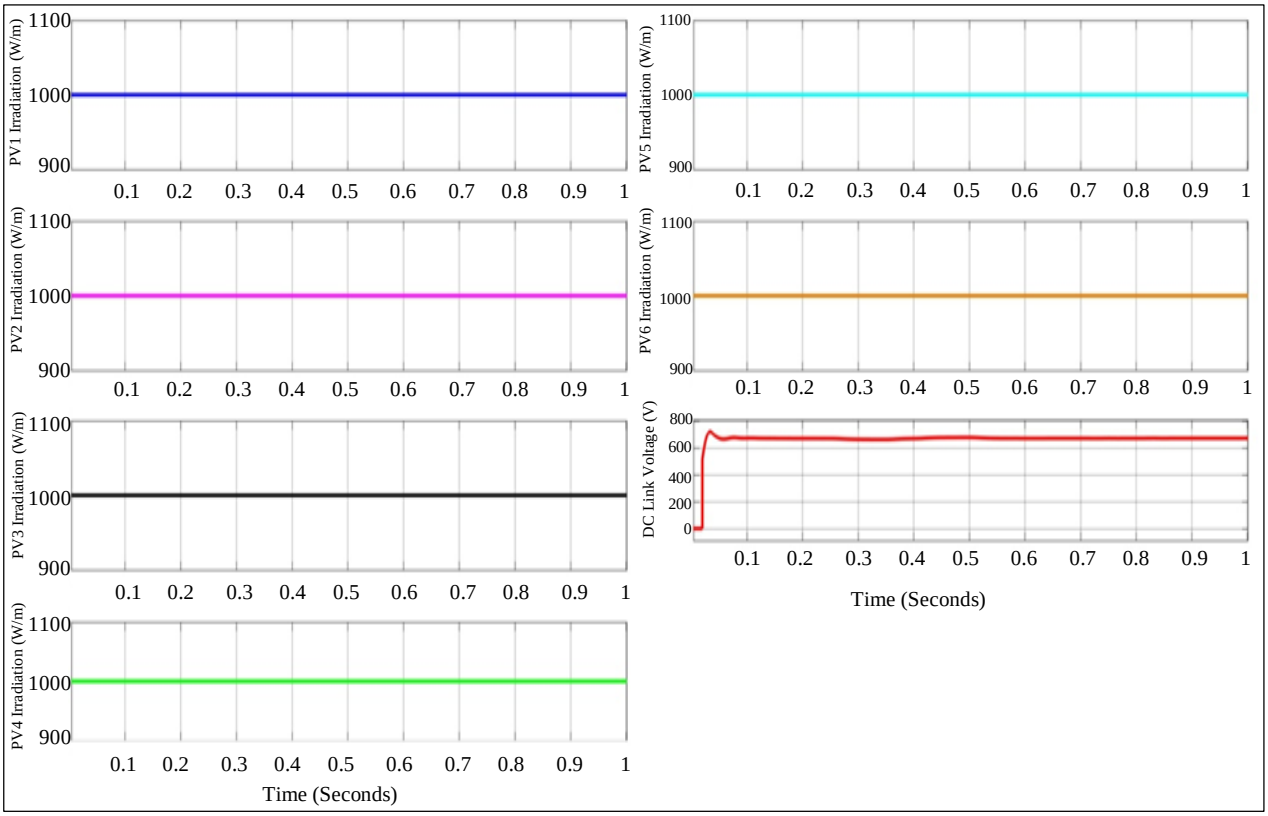

(c) G, SDCV

Fig. 11 Signals for case-1

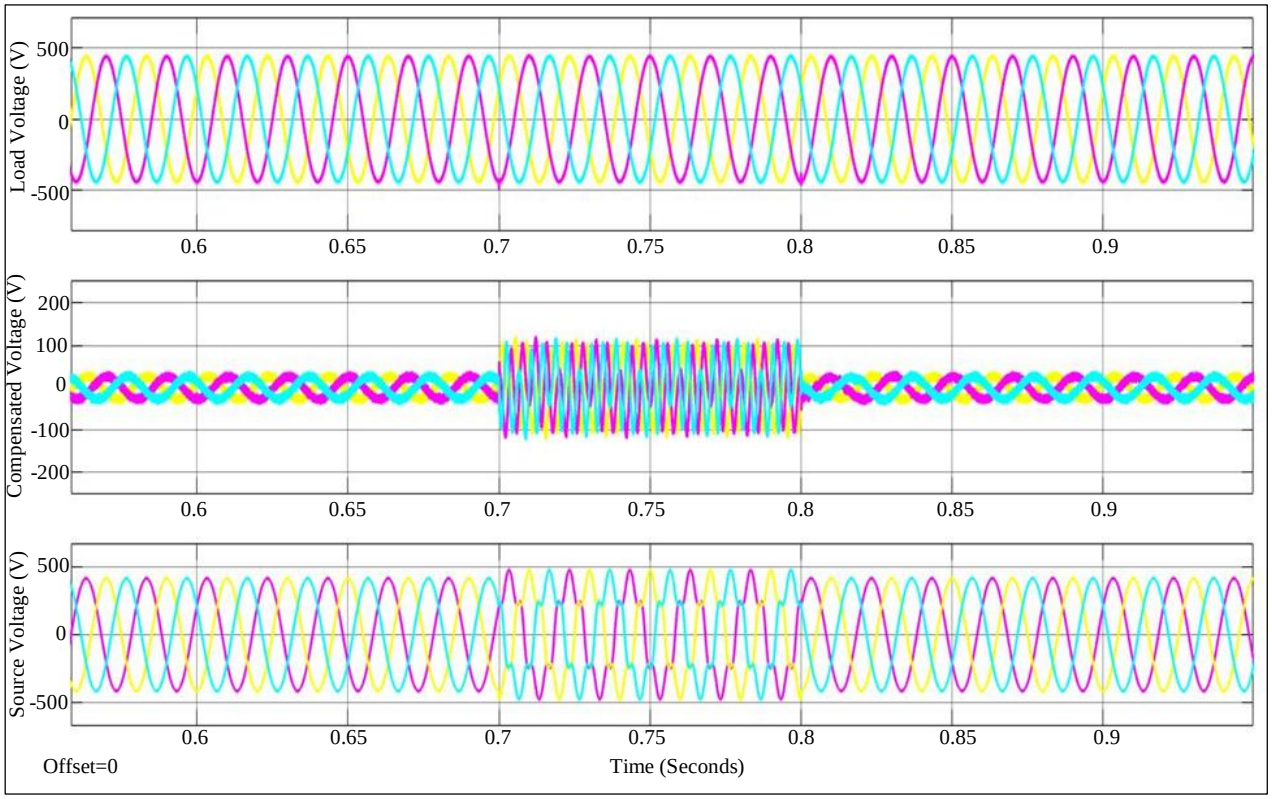

(a) Source, injected and demand voltages

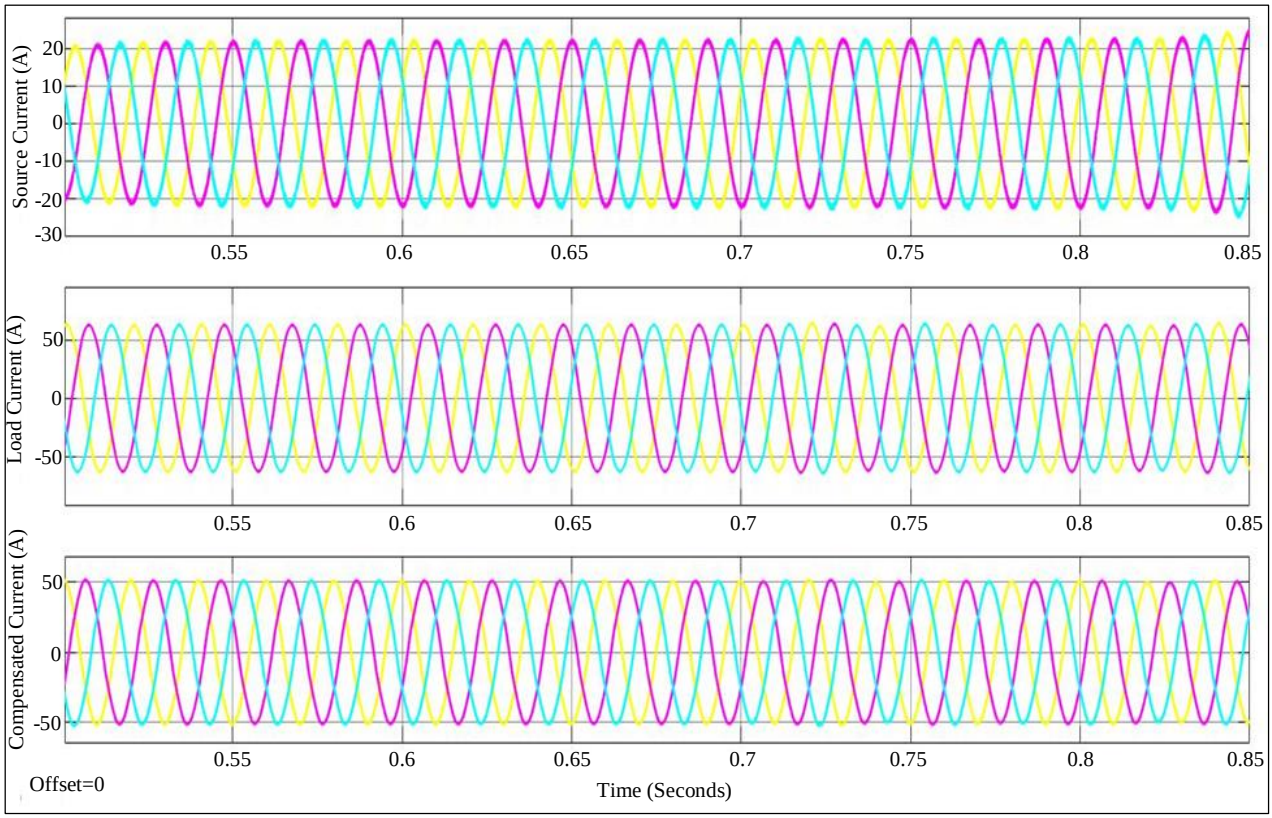

(b) Source, demand, and injected currents

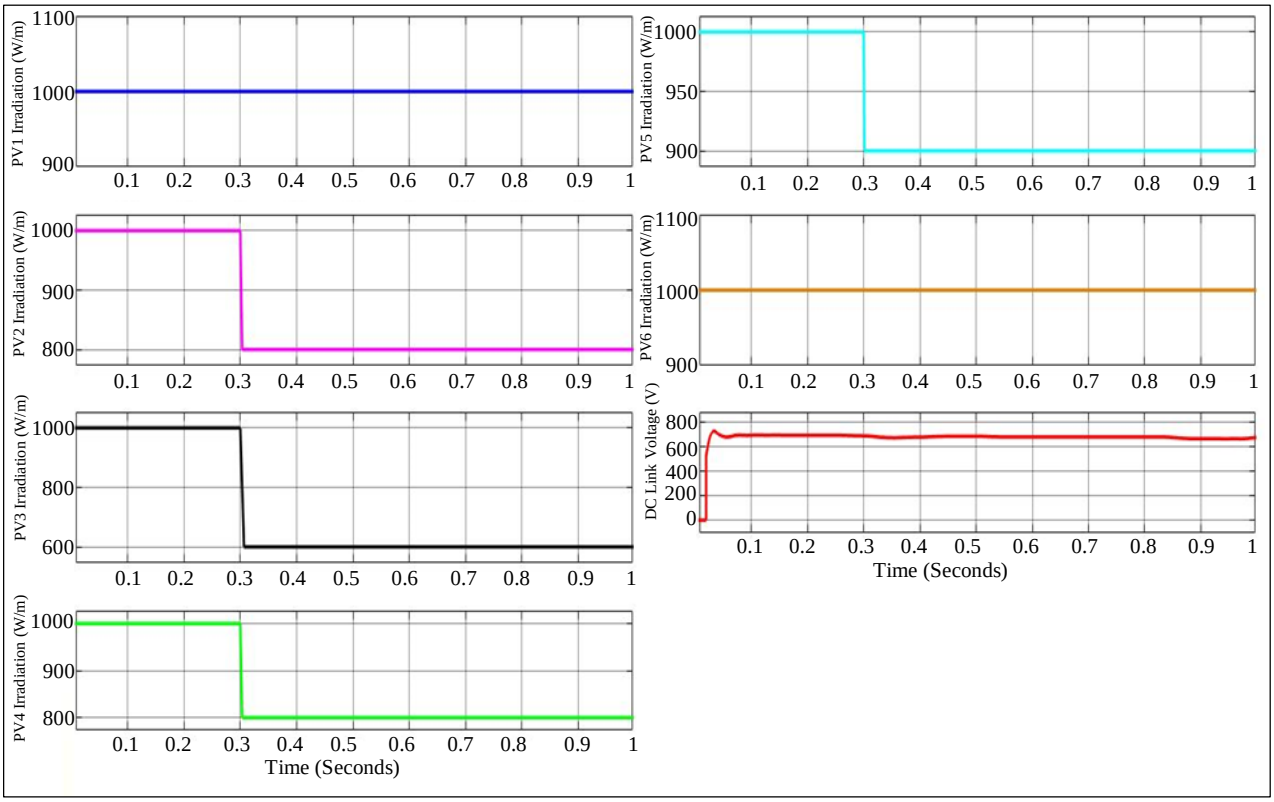

(c) G, SDCV

Fig. 12 Signal for case-2

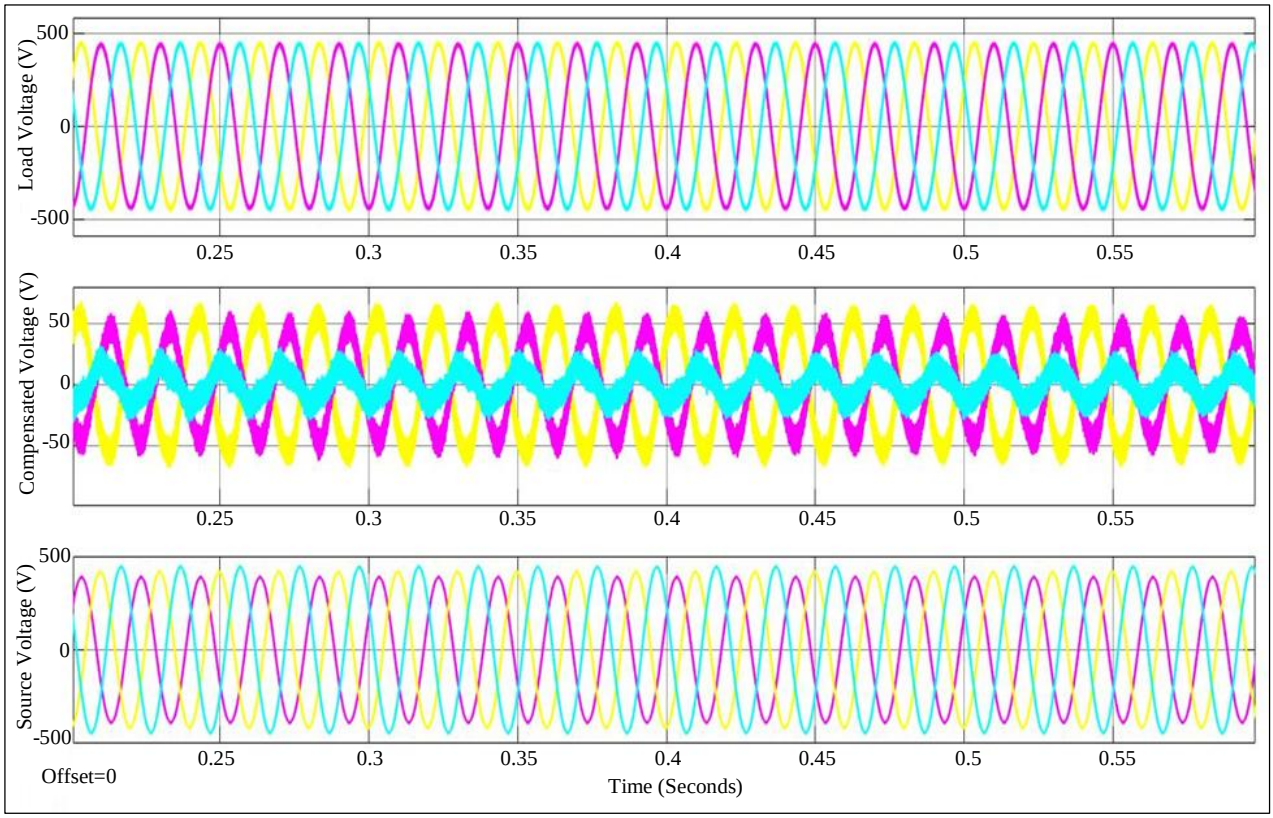

(a) Source, injected and demand voltages

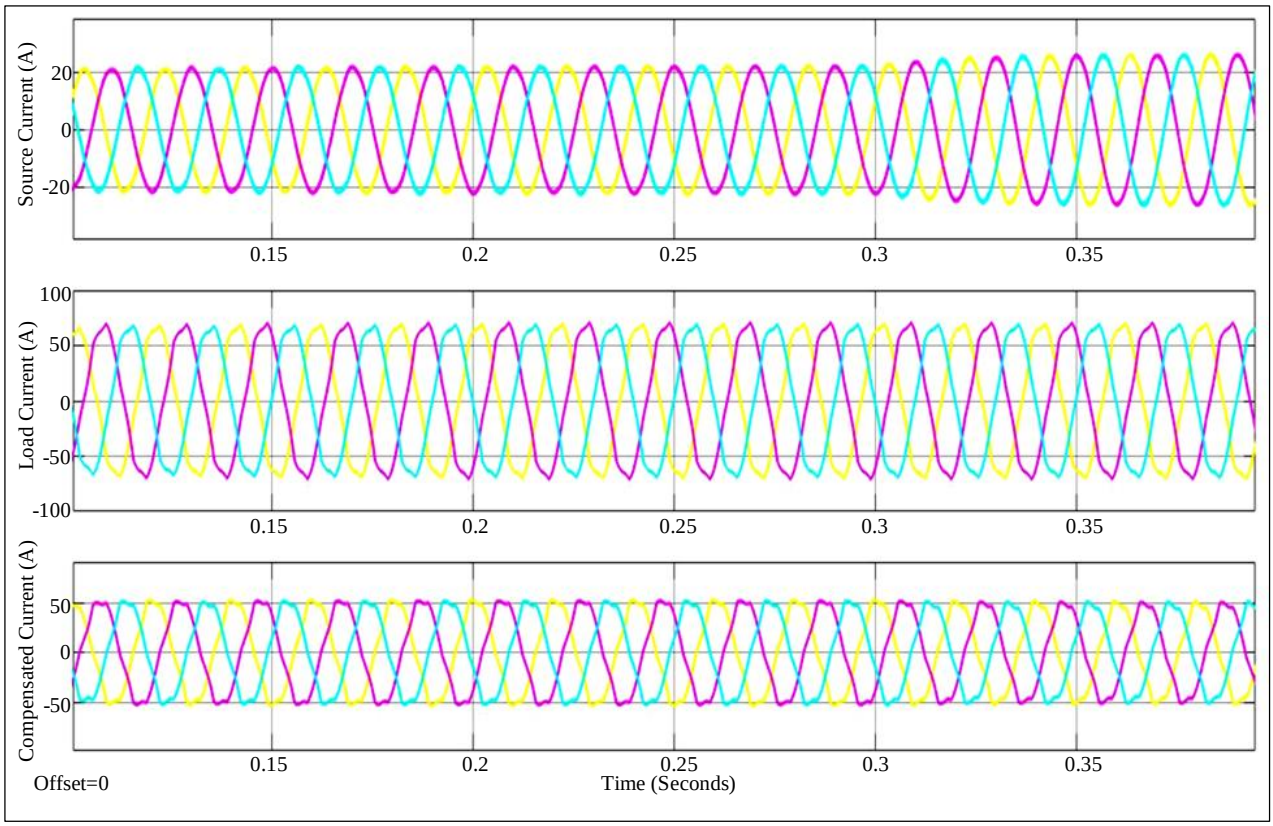

(b) Source, demand, and injected currents

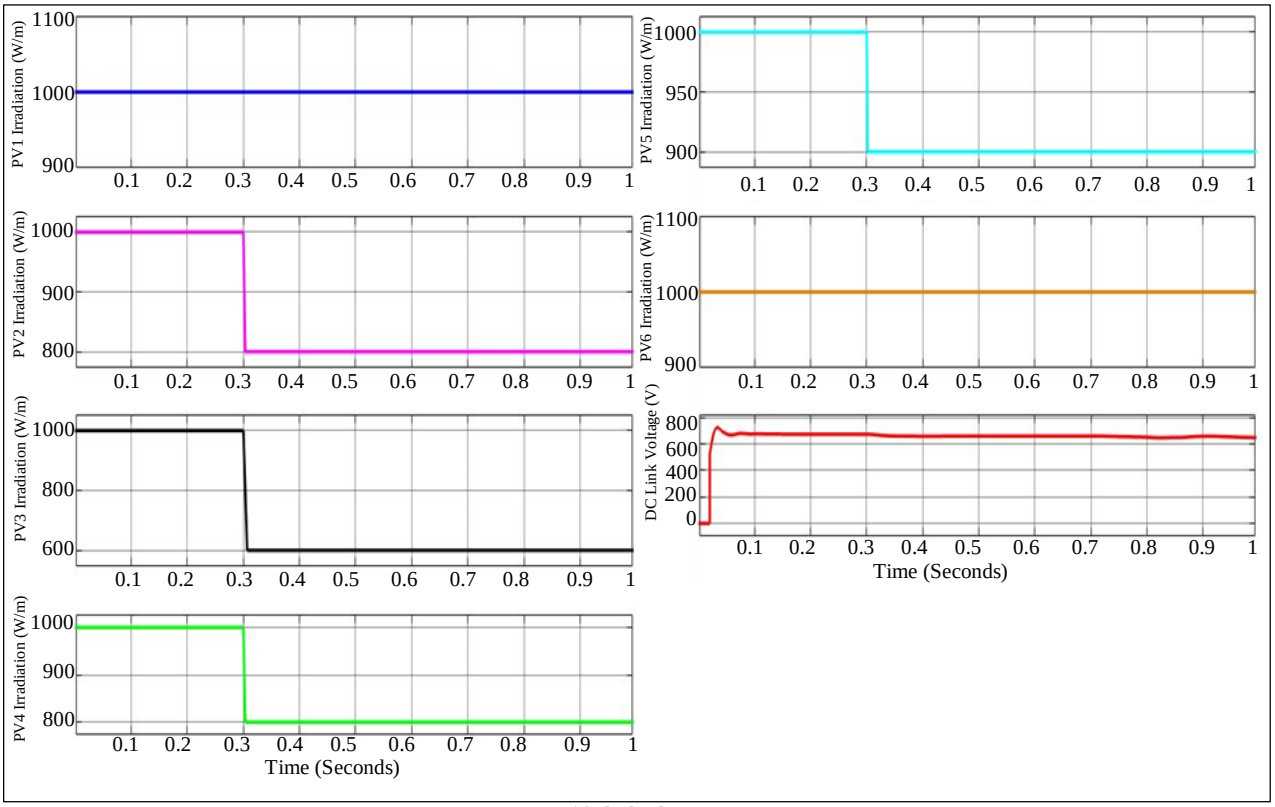

(c) G, SDCV

Fig. 13 Signal for case-3

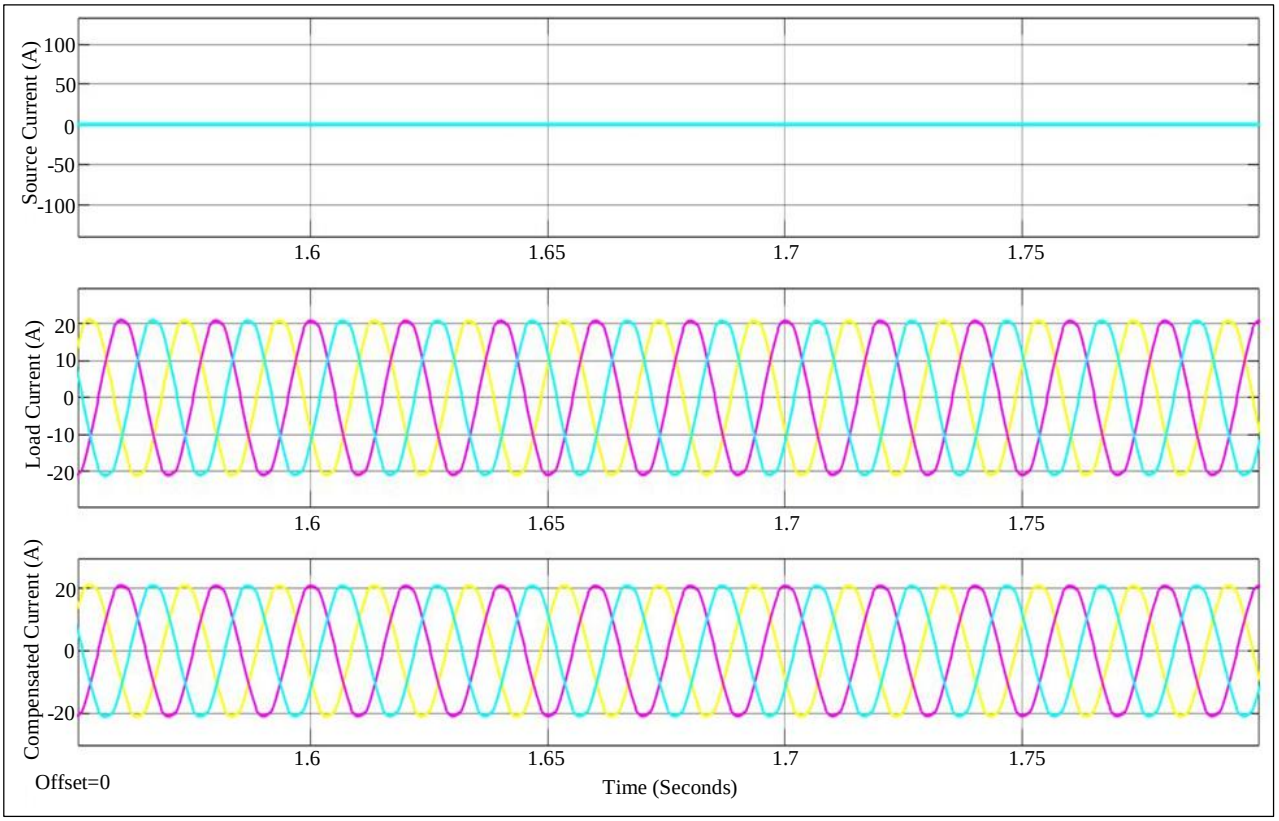

(a) Source, Demand, and Injected currents

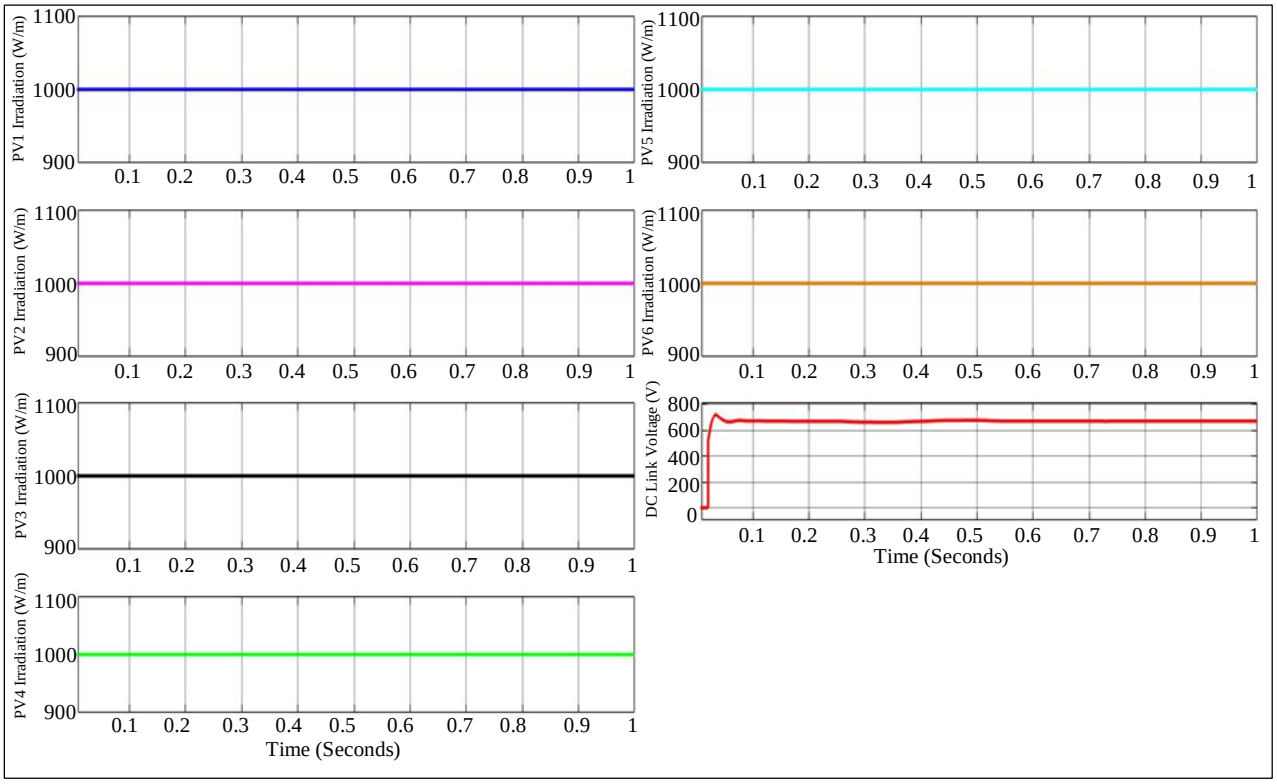

(b) G, SDCV

Fig. 14 signals for case-4

As seen in Figure 13(a), case 3's concurrent operation of loads 4, 3 and 1 within balanced phase V_S. It was found that the current at the load was severely distorted harmonically, unbalanced, and irregular in shape, as Figure 13(b) illustrates. The suggested controller can effectively balance the V_{dc} in 0.05 seconds during sun irradiation and load fluctuation, as shown in Figure 13(c). This is a significant reduction in comparison to all case studies. THD is likewise decreased to 1.84%. As seen in Figure 14(a), case 4, VS is considered to be out of balance. The technology suppresses voltage-phase imbalances and provides stable voltage to the load. In this instance, the system is islanded, meaning that the load is supplied by the solar and battery systems.

Here, it is seen to be unbalanced yet sinusoidal in shape in Figure 14(b). Furthermore, as illustrated in Figure 14(c), it is capable of continuously radiating while controlling the Vdc in an islanded scenario. Figure 15 shows the spectrum analysis of the established approach for considered tests. Figure 16 makes it abundantly evident that the suggested method takes far less time (in seconds) than conventional ways to achieve a stable DC bus capacitor voltage.

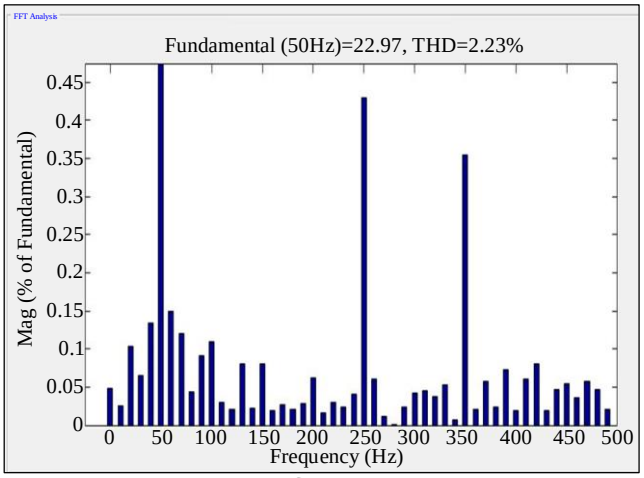

Case 1

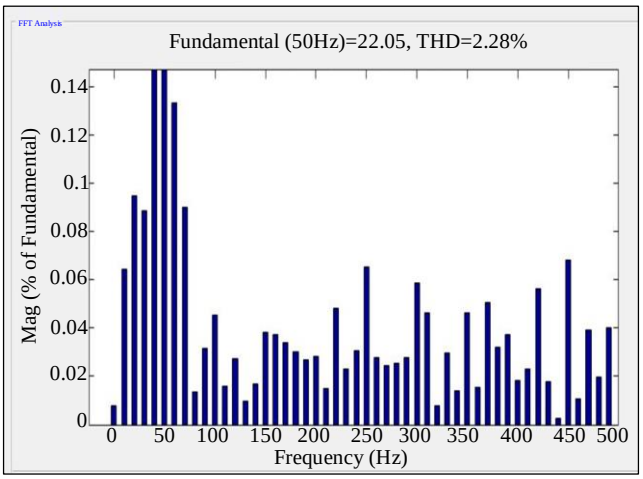

Case 2

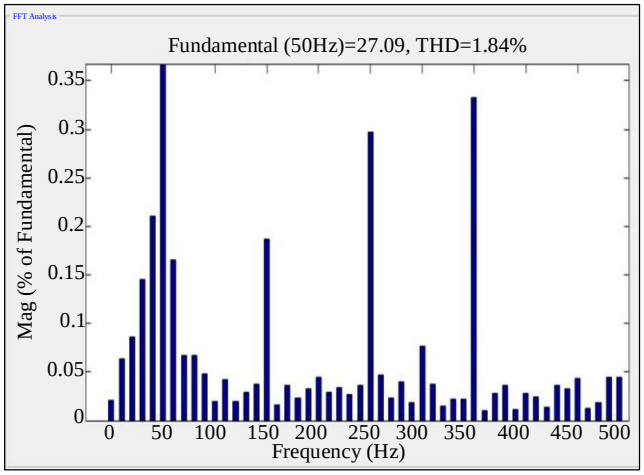

Case 3

Fig. 15 FFT analysis

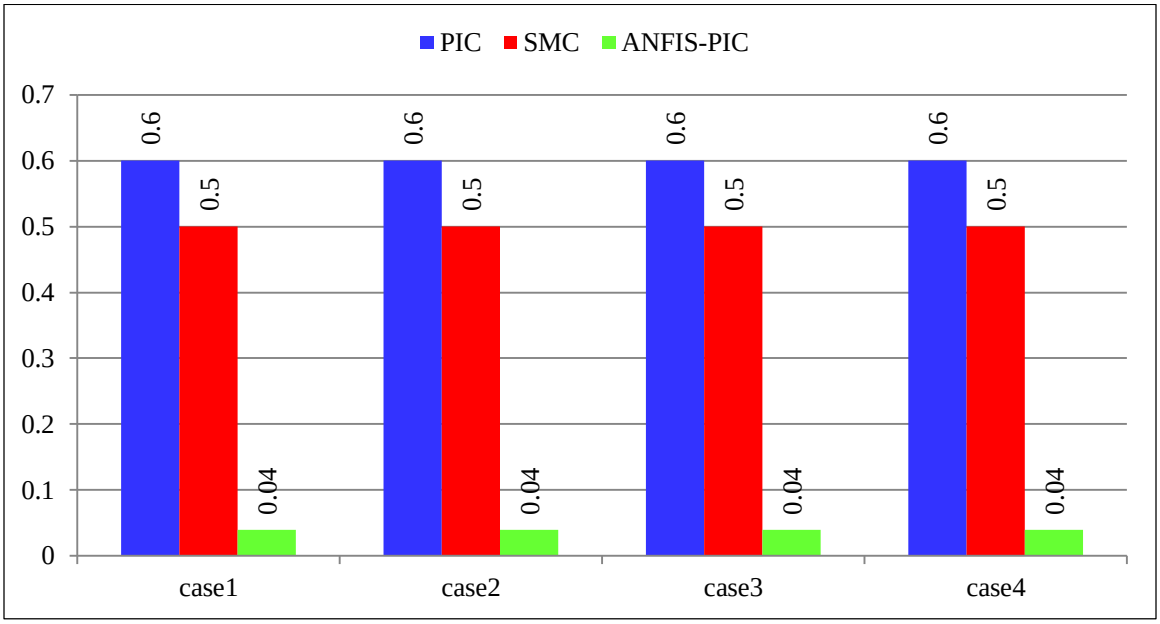

Fig. 16 DC bus capacitor voltage settling time

6. Conclusion

To efficiently maintain DC bus capacitor voltage despite load and solar radiation changes, the ANFIS-PIC control for SHAF and the BES control for UPQC were developed in tandem. In order to minimize THD, this design goal entails removing voltage signal harmonics, swell, and sag produced in the source voltage and minimizing flaws in the current waveform morphologies. It is clear from analyzing the ability of the developed technique on four test studies that it greatly lowers THD and efficiently provides power to the demand in standalone circumstances. Moreover, a comparative study using conventional PIC, SMC, and controllers covered in the review shows that the suggested controller outperforms the others in terms of performance. It is clear from the analysis of the performance of the proposed approach in 4 cases successfully lowers the THD to 2.23%, 2.28%, and 1.84%. The outcomes unequivocally show that the suggested method successfully brought the THD down to manageable levels. One possible direction for future research is to look further at the suggested Multi-level UPQC system.

References

[1] N.C. Sai Sarita, S. Suresh Reddy, and P. Sujatha, "Control Strategies for Power Quality Enrichment in Distribution Network Using UPQC," *Materials Today: Proceedings*, vol. 80, pp. 2872-2882, 2023. [CrossRef] [Google Scholar] [Publisher Link]

[2] S. Poongothai, and S. Srinath, "Power Quality Enhancement in Solar Power with Grid Connected System Using UPQC," *Microprocessors and Microsystems*, vol. 79, 2020. [CrossRef] [Google Scholar] [Publisher Link]

[3] N. Gowtham, and Shobha Shankar, "UPQC: A Custom Power Device for Power Quality Improvement," *Materials Today: Proceedings*, vol. 5, no. 1, pp. 965-972, 2018. [CrossRef] [Google Scholar] [Publisher Link]

[4] A. Senthil Kumar, S. Rajasekar, and P. Ajay-D-Vimal Raj, "Power Quality Profile Enhancement of Utility Connected Microgrid System Using ANFIS-UPQC," *Procedia Technology*, vol. 21, pp. 112-119, 2015. [CrossRef] [Google Scholar] [Publisher Link]

[5] Sarita Samal, and Prakash Kumar Hota, "Design and Analysis of Solar PV-Fuel Cell and Wind Energy Based Microgrid System for Power Quality Improvement," *Cogent Engineering*, vol. 4, no. 1, 2017. [CrossRef] [Google Scholar] [Publisher Link]

[6] Subanth Williams A., Suja Mani Malar R., and Ahilan T., "Wind Connected Distribution System with Intelligent Controller Based Compensators for Power Quality Issues Mitigation," *Electric PowerSystems Research*, vol. 217, 2023. [CrossRef] [Google Scholar] [Publisher Link]

[7] Udaya K. Renduchintala et al., "ANFIS-Fuzzy Logic Based UPQC in Interconnected Microgrid Distribution Systems: Modeling, Simulation and Implementation," *Journal of Engineering*, vol. 2021, no. 1, pp. 6-18, 2021. [CrossRef] [Google Scholar] [Publisher Link]

[8] C. Pazhanimuthu, and S. Ramesh, "Grid Integration of Renewable Energy Sources (RES) for Power Quality Improvement Using Adaptive Fuzzy Logic Controller Based Series Hybrid Active Power Filter (SHAPF)," *Journal of Intelligent & Fuzzy Systems*, vol. 35, no. 1, pp. 749-766, 2018. [CrossRef] [Google Scholar] [Publisher Link]

[9] Aruchamy Sakthivel et al., "Experimental Investigations on Ant Colony Optimized PI Control Algorithm for Shunt Active Power Filter to Improve Power Quality," *Control Engineering Practice*, vol. 42, pp. 153-169, 2015. [CrossRef] [Google Scholar] [Publisher Link]

[10] S.S. Dheeban, and N.B. Muthu Selvan, "ANFIS-Based Power Quality Improvement by Photovoltaic Integrated UPQC at Distribution System," *IETE Journal of Research*, vol. 69, no. 5, pp. 2353-2371, 2023. [CrossRef] [Google Scholar] [Publisher Link]

[11] D. Krishna, M. Sasikala, and V. Ganesh, "Adaptive FLC-Based UPQC in Distribution Power Systems for Power Quality Problems," *International Journal of Ambient Energy*, vol. 43, no. 1, pp. 1719-1729, 2022. [CrossRef] [Google Scholar] [Publisher Link]

[12] K.R. Suja, and I.J. Raglend, "Adaptive Genetic Algorithm/Neuro-Fuzzy Logic Controller Based Unified Power Quality Conditioner Controller for Compensating Power Quality Problems," *Australian Journal of Electrical and Electronics Engineering*, vol. 10, no. 3, pp. 351-361, 2013. [Google Scholar] [Publisher Link]

[13] Shashi Gandhar, Jyoti Ohri, and Mukhtiar Singh, "A Mathematical Framework of ANFIS Tuned UPQC Controlled RES Based Isolated Microgrid System," *Journal of Interdisciplinary Mathematics*, vol. 25, no. 5, pp. 1467-1477, 2022. [CrossRef] [Google Scholar] [Publisher Link]

[14] Sudheer Vinnakoti, and Venkata Reddy Kota, "Performance Analysis of ANN-Based Multilevel UPQC under Faulty and Overloading Conditions," *International Journal of Ambient Energy*, vol. 42, no. 13, pp. 1516-1528, 2021. [CrossRef] [Google Scholar] [Publisher Link]

[15] Joyal Isac Sankar, and Srinath Subbaraman, "Multi-Converter UPQC Optimization for Power Quality Improvement Using Beetle Swarm-Based Butterfly Optimization Algorithm," *Electric Power Components and Systems*, vol. 51, no. 20, pp. 2487-2498, 2023. [CrossRef] [Google Scholar] [Publisher Link]

[16] Shravan Kumar Yadav, B. Sabitha, and Anush Prabhakaran, "Optimal Placement of UPQC in Distribution Network Using Hybrid Approach," *Cybernetics and Systems*, vol. 54, no. 7, pp. 1014-1036, 2023. [CrossRef] [Google Scholar] [Publisher Link]

[17] Jianxun Jin et al., "An Improved Compensation Method for Voltage Sags and Swells of the Electric Vehicles Charging Station Based on a UPQC-SMES System," *International Journal of Electrical Power & Energy Systems*, vol. 143, 2022. [CrossRef] [Google Scholar] [Publisher Link]

[18] Mallikarjuna Golla, S. Sankar, and K. Chandrasekaran, "Renewable Integrated UAPF Fed Microgrid System for Power Quality Enhancement and Effective Power Flow Management," *International Journal of Electrical Power & Energy Systems*, vol. 133, 2021. [CrossRef] [Google Scholar] [Publisher Link]

[19] T. Arulkumar, and N. Chandrasekaran, "Development of Improved Sparrow Search-Based PI Controller for Power Quality Enhancement Using UPQC Integrated with Medical Devices," *Engineering Applications of Artificial Intelligence*, vol. 116, 2022. [CrossRef] [Google Scholar] [Publisher Link]

[20] A. Senthilkumar, and P. Ajay-D-Vimal Raj, "ANFIS and MRAS-PI Controllers Based Adaptive-UPQC for Power Quality Enhancement Application," *Electric Power Systems Research*, vol. 126, pp. 1-11, 2015. [CrossRef] [Google Scholar] [Publisher Link]

[21] Koganti Srilakshmi et al., "A Renewable Energy Source Fed Neuro-Fuzzy Controlled Multilevel UPQC for Power Quality Improvement," *International Journal of Renewable Energy Research*, vol. 14, no. 2, pp. 370-385, 2024. [CrossRef] [Google Scholar] [Publisher Link]

[22] Koganti Srilakshmi et al., "Development of AI Controller for Solar /Battery Fed H-Bridge Cascaded Multilevel Converter UPQC under Different Loading Conditions," *International Journal of Renewable Energy Research*, vol. 14, no. 2, pp. 403-417, 2024. [CrossRef] [Google Scholar] [Publisher Link]

[23] Koganti Srilakshmi et al., "Design and Performance Analysis of Fuzzy Based Hybrid Controller for Grid Connected Solar-Battery Unified Power Quality Conditioner," *International Journal of Renewable Energy Research*, vol. 13, no. 1, pp. 1-13, 2023. [CrossRef] [Google Scholar] [Publisher Link]

[24] Koganti Srilakshmi et al., "Performance Analysis of Artificial Intelligence Controller for PV and Battery Connected UPQC," *International Journal of Renewable Energy Research*, vol. 13, no. 1, pp. 155-170, 2023. [CrossRef] [Google Scholar] [Publisher Link]

[25] Koganti Srilakshmi et al., "Design and Performance Analysis of Hybrid Controller for Self Tuning Filter Based Solar Integrated UPQC," *International Journal of Renewable Energy Research*, vol. 13, no. 1, pp. 1250-1259, 2023. [CrossRef] [Google Scholar] [Publisher Link]

[26] Sravanthy Gaddameedhi et al., "Hybrid Controller Based Solar-Fuel Cell Integrated UPQC for Power Quality Enhancement," *International Journal of Renewable Energy Research*, vol. 11, no. 4, pp. 1673-1683, 2021. [CrossRef] [Google Scholar] [Publisher Link]

[27] Koganti Srilakshmi et al., "Design of Soccer League Optimization Based Hybrid Controller for Solar-Battery Integrated UPQC," *IEEE Access*, vol. 10, pp. 107116-107136, 2022. [CrossRef] [Google Scholar] [Publisher Link]

[28] Koganti Srilakshmi et al., "Green Energy-Sourced AI-Controlled Multilevel UPQC Parameter Selection Using Football Game Optimization," *Frontiers in Energy Research*, vol. 12, 2024. [CrossRef] [Google Scholar] [Publisher Link]

[29] Koganti Srilakshmi et al., "Optimal Design of Solar/Wind/Battery and EV Fed UPQC for Power Quality and Power Flow Management Using Enhanced Most Valuable Player Algorithm," *Frontiers in Energy Research*, vol. 11, 2024. [CrossRef] [Google Scholar] [Publisher Link]

[30] Koganti Srilakshmi et al., "Development of Renewable Energy Fed Three-Level Hybrid Active Filter for EV Charging Station Load Using Jaya Grey Wolf Optimization," *Scientific Reports*, vol. 14, 2024. [CrossRef] [Google Scholar] [Publisher Link]

[31] Alapati Ramadevi et al., "Optimal Design and Performance Investigation of Artificial Neural Network Controller for Solar- and Battery-Connected Unified Power Quality Conditioner," *International Journal of Energy Research*, 2023. [CrossRef] [Google Scholar] [Publisher Link]

[32] Koganti Srilakshmi et al., "Simulation of Grid/Standalone Solar Energy Supplied Reduced Switch Converter with Optimal Fuzzy Logic Controller Using Golden Ball Algorithm," *Frontiers in Energy Research*, vol. 12, 2024. [CrossRef] [Google Scholar] [Publisher Link]

[33] Koganti Srilakshmi et al., "Multi objective Neuro-Fuzzy Controller Design and Selection of Filter Parameters of UPQC Using Predator Prey Firefly and Enhanced Harmony Search Optimization," *International Transactions on Electrical Energy Systems*, 2024. [CrossRef] [Google Scholar] [Publisher Link]

[34] Koganti Srilakshmi et al., "Optimization of ANFIS Controller for Solar/Battery Sources Fed UPQC Using an Hybrid Algorithm," *Electrical Engineering*, vol. 106, pp. 3743-3770, 2024. [CrossRef] [Google Scholar] [Publisher Link]

[35] Koganti Srilakshmi et al., "A New Control Scheme for Wind/Battery Fed UPQC for the Power Quality Enhancement: A Hybrid Technique," *IETE Journal of Research*, 2024. [CrossRef] [Google Scholar] [Publisher Link]

[36] Koganti Srilakshmi, Arun Nambi Pandian, and Aravindhababu Palanivelu, "Fuzzy Based Hybrid Controller for UPQC with Wind and Battery Storage Systems," *International Journal of Electronics*, 2023. [CrossRef] [Google Scholar] [Publisher Link]

Appendix-1: Parameters of Proposed System

The parameter values of system considered: supply voltage= 415 V, frequency=50 Hz; Harmonic load-1: Rectifier bridge R= 30Ω, and L=20mH; active reactive power load-2: active power=1000W, Reactive power=1000Vars ; Un equal phases load-3: R1= 10, R2=20 & R3=15ohm; L1=9.50mH, L2=10.50 mH&L3=18.50 mH ; EV charging station load-4: battery 48*8=384Wh ; V_{dc}= 700 V; C_{dc}= 2200 µF; L_{sh}: 12.5mH; R_{sh}: 1ohm; C_{se}: 60µF.

Appendix-2: EV and Solar Parameters

SPR-305E -WHT-D; Np/Ns= 11/5; max P_{PV}: 305.226W; I_{PV}= 5.58A; OCV: 64.2 V; SCC: 5.96A; Battery: voltage= 500 v; state of charge= 60%; capacity: 100Ah.

Nomenclature:

PQ	Power Quality
EVCS	EV Charging Station
NNC	Neural Network Controller
FLC	Fuzzy Logic Controller
ANFIS	Artificial Neuro Fuzzy Interface System
SPVS	Solar PV Systems
UPQC's	Unified Power Quality Conditioner Device
PIC	Proportional Integral Controller
SVDC	Steady DC Capacitance Voltage
THD	Total Harmonic Distortion
BESD	Battery Energy Storage Device
PLL	Phase-Locked Loop
SHPF, SEAF	Shunt and Series Active Power Filters

ACO	Ant Colony Optimization
DCLV	DC Link Voltage
GA	Genetic Algorithm
VSC	Voltage Source Converter
PB	Positive Big
ANFIS-PIC	ANFIS integrated PIC hybrid technique
E	Error
CE	Change of Error
EV	Electric Vehicle
PM	Positive Medium
NM	Negative Medium
SSA	Sparrow Search Algorithm
NB	Negative Big
NS	Negative Small
PS	Positive Small
Rs, PV, Rsh, PV	Series and parallel cell resistors
ZO	Zero
iPV, ish, PV	Current in PV
id	Forward diode current
iph	Sunlight photo current
M	Module
G	Irradiation
T	Temperature
VPV and PPV	PV output voltage and power
ΔI, ΔV	Change in current and voltage
Np, Ns	No of parallel and series modules
Q	Battery charge and irefB Battery current and reference current
SOC max, SOC min	Limits of SOC
VB, CB, LB	Batteries voltage, capacitance and inductance